



SYNTHETIC EARTHQUAKE GROUND MOTIONS AT CLOSELY SPACED DISTANCES WITH SYNACC

Maria I. Todorovska¹, Mihailo D. Trifunac², Vincent W. Lee² and Nebojša Orbović³

¹Research Professor, Dept. of Civil Engineering, U. Southern. California, Los Angeles, CA
(mtodorov@usc.edu)

²Professor, Dept. of Civil Engineering, U. Southern California, Los Angeles, CA (trifunac@usc.edu;
vlee@usc.edu)

³Canadian Nuclear Safety Commission, Ottawa, Ontario (Nebojsa.Orbovic@cnsccsn.gc.ca)

ABSTRACT

This paper presents a brief review of the SYNACC method for synthesizing earthquake ground motion time histories on an array of points in space. SYNACC is a combination of an empirical and physical model-based method, and involves unfolding in time a site-specific Fourier amplitude spectrum of ground acceleration obtained for a scenario earthquake by an empirical scaling model. The unfolding consists of representing the ground motion as a superposition of traveling surface Love and Rayleigh waves and of body P and S waves, which propagate with phase and group velocities consistent with the dispersion characteristic of the site geology, approximated by parallel layers. Because the coefficients of expansion are scaled so that the Fourier spectrum of the synthetic motion matches a site specific empirical spectrum, the synthetic motions are consistent statistically with observations within the recording range of typical accelerographs (0.02-25 Hz). A Uniform Hazard Fourier spectrum or any specified Fourier spectrum can also be used as a target spectrum. The output consists of synthetic accelerations, velocities and displacements, and point strains, rotations and curvatures, all at a point or at an array of points. Such time histories are useful for the design of spatially extended structures, like pipelines, bridges and tunnels.

INTRODUCTION

Time histories of strong ground motion are often required as input to structural models for nonlinear response analyses of structures. As the number of strong motion records for design is limited, and the number of records for particular site conditions is even more limited, records from other geologic regions are often used. Flexible and long structures, which have characteristic length comparable to or longer than the wavelengths of the strong ground motion selected for design, are sensitive also to the ground strains and differential motion of their supports, and require time histories of ground motion specified at an array of closely spaced points. Typical examples of such structures are pipelines, bridges and tunnels (Fig. 1). As the number of dense accelerograph arrays worldwide is small, the number of such earthquake observations is limited. Synthetic *site-specific* motions with the desired characteristics are an alternative to using actual earthquake records from other, sometimes very different, geologic regions.

This paper presents an overview of the SYNACC method for generating multi-component synthetic ground motion time histories, and its extension to motions on an *array of points* on the ground surface (Todorovska et al., 2013). SYNACC combines empiricism and physical model based simulation, and does not belong to either of the two main groups of methods - engineering stochastic and seismological physics based - for synthesizing spatially correlated strong ground motions (see review on this topic in Zerva, 2009). SYNACC advantage over the stochastic methods is that it does not rely on simplified coherency functions obtained from other regions and it is fully nonstationary. Its advantage over the seismological methods is that it is by construction calibrated, i.e. consistent in statistical sense with observations, and over a broader frequency band (0.02-25 Hz).

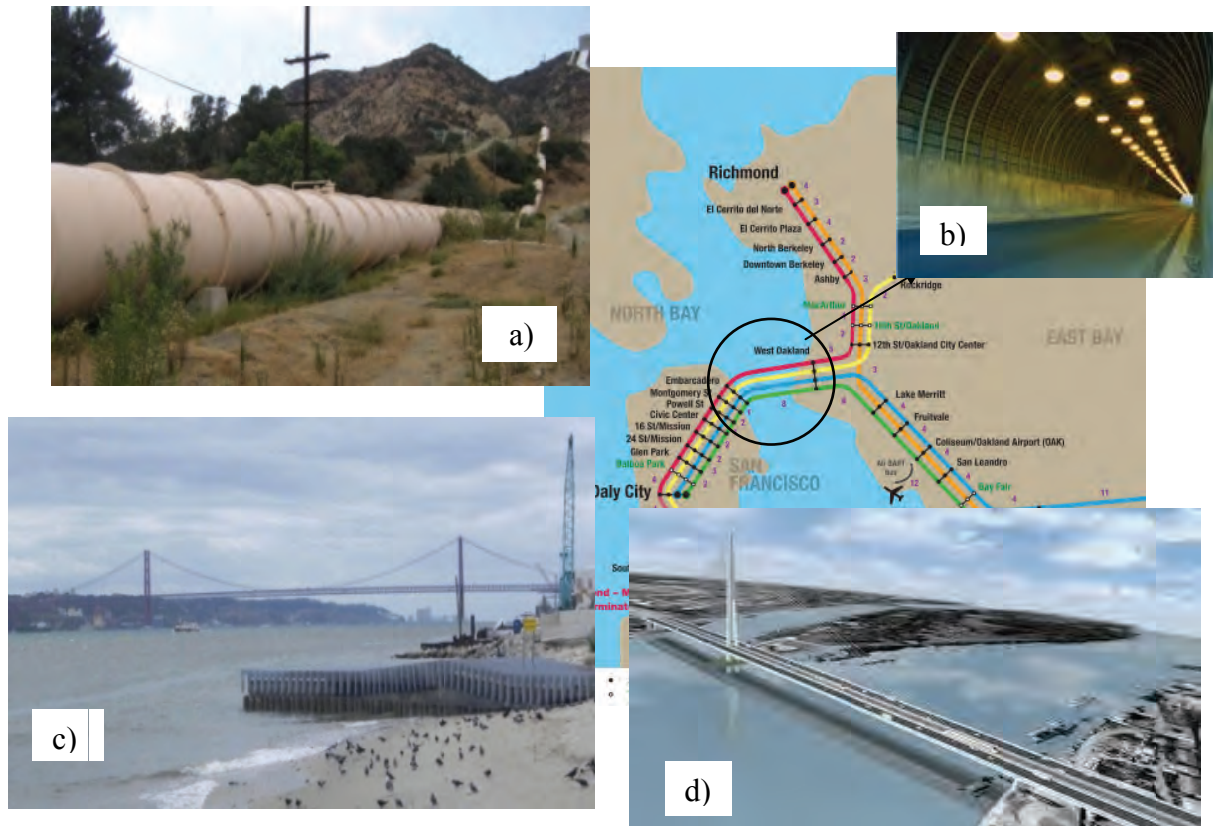


Fig. 1 Examples of long structures. a) Water pipe (photo by Craig Davis); b) Transbay Tube - part of BART, 5.8 km long, runs under San Francisco Bay in California (www.bart.gov); c) Ponte 25 de Abril (Tagus Bridge), Lisbon, Portugal, 1,033 m main span (photo by M. Todorovska); d) Ada Bridge in Belgrade, Serbia, total length 996 m, longest span 376 m (photo by M. Trifunac).

The SYNACC method was first proposed by Trifunac (1971) and demonstrated for a site in Imperial Valley in Southern California. The method evolved over the years, by inclusion of more current empirical scaling laws for Fourier amplitude spectra of acceleration and frequency dependent duration (Wong and Trifunac, 1978,1979; Trifunac and Lee, 1985), and extension to prediction of rotational motions (Lee and Trifunac, 1985a, 1987), strains (Lee, 1990) and curvature (Trifunac, 1990), all at a point in space (see also review in Lee, 2002). Details about its extension to array of points can be found in Todorovska et al. (2013).

METHODOLOGY

The SYNACC method is based on the assumption that the seismic waves from the source arrive at the site via surface and body waves, which follow different paths and are attenuated differently, but the *total* motion can be predicted *reliably*, in a statistical sense, using empirical scaling laws for Fourier amplitude spectra of acceleration. It is also assumed that the geology *near* the site can be represented as a set of parallel layers. The surface waves (Love and Rayleigh) arrive horizontally through the low velocity layers with velocities that are frequency dependent, while the body waves arrive from depth at an angle, which is close to vertical for soft geology near the surface. This is illustrated schematically in Fig. 2 showing the earthquake fault, the surface and body waves, and a segment of a pipeline (representing a long structure) located on sediments.

Synthetic Motions at a Point

Following these assumptions, the empirically predicted Fourier amplitude spectrum (0-25 Hz) is partitioned into N narrow non-overlapping sub-bands, and the energy in each sub-band is partitioned among surface and body waves. The waves in a narrow sub-band propagate as a group, forming a wavelet packet, the envelope of which propagates with the group velocity $U_m(\omega)$, while the individual components propagate with their phase velocities $c_m(\omega)$. The total motion (acceleration in this case, because it is predicted by empirical scaling laws), therefore, is represented as a superposition of such wavelet packets

$$\ddot{u}(x,t) = \sum_{n=1}^N \sum_{m=1}^{M_n} A_{nm}^* w_{nm}(x;t) \quad (1)$$

where

$$w_{nm}(x;t) = \text{sinc} \left[\Delta\omega_n \left(t - \frac{x}{U_{nm}} \right) \right] \exp [i(\omega_n t - k_{nm} x)] \quad (2)$$

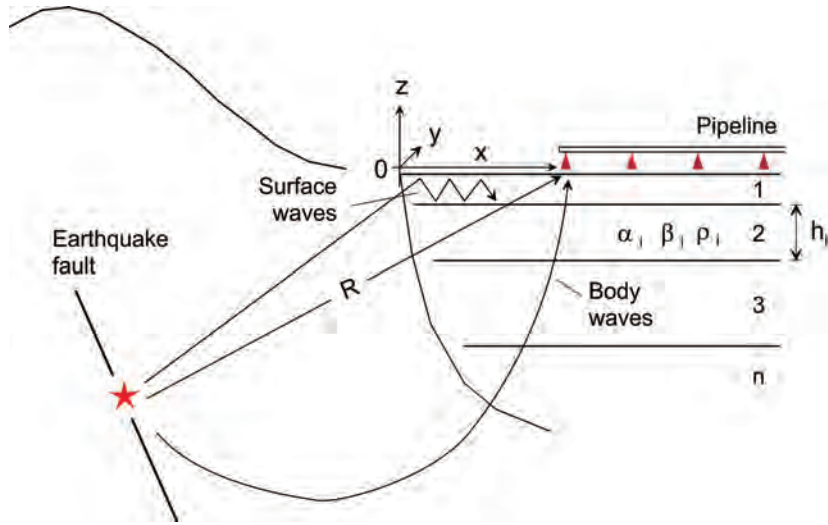


Fig. 2 Model.

is the wavelet packet with

$$k_{nm} = \frac{\omega_n}{c_{nm}} \left(1 - i \frac{1}{2Q} \right) \quad (3)$$

being the complex horizontal wave number. In Eqn. (3), Q is the quality factor, assumed to be constant (Trifunac, 1994), and A_{nm}^* are complex valued coefficients of expansion. The summation is over frequency bands (index n) and also over different propagation modes (index m), which are branches of the surface waves. The body waves, P and S, are treated as two additional modes. The horizontal phase velocities of the surface waves are obtained from dispersion analysis of the medium (Haskell 1953). The Fourier transform of the wavelet $w_{nm}(x;t)$ is

$$\hat{w}_{nm}(x; \omega) = \frac{\pi}{\Delta\omega_n} \exp \left[-i \left(\frac{\omega - \omega_n}{U_{nm}} + k_{nm} \right) x \right] p_{\Delta\omega_n}(\omega - \omega_n) \quad (4)$$

The coefficients of the expansion in Eqn (1) are determined so that the Fourier spectrum amplitudes of the synthetic motions match those of a target spectrum, discussed later in this paper. However, for particular site geology, they are related, and their relative amplitudes depend on the frequency and mode number. In the illustrations presented in this paper, we use a variant of the geology profile for a site in Imperial Valley studied by Trifunac (1971) and the same relationship between the coefficients as derived in that study. The profile is shown in Fig. 3. The coefficients A_{nm}^* also contain a random phase factor, which is the phase of the packet at a chosen reference point between the epicenter and the site, $x = 0$ in Fig. 1, from where the parallel layers geology is adopted to be representative of the wave path, referred to as “edge of the valley”. It is an abstraction introduced to avoid excessively long duration of the synthetic motion, and is discussed in Todorovska et al. (2013). The x -coordinate of the site, in general, is different from the epicentral distance.

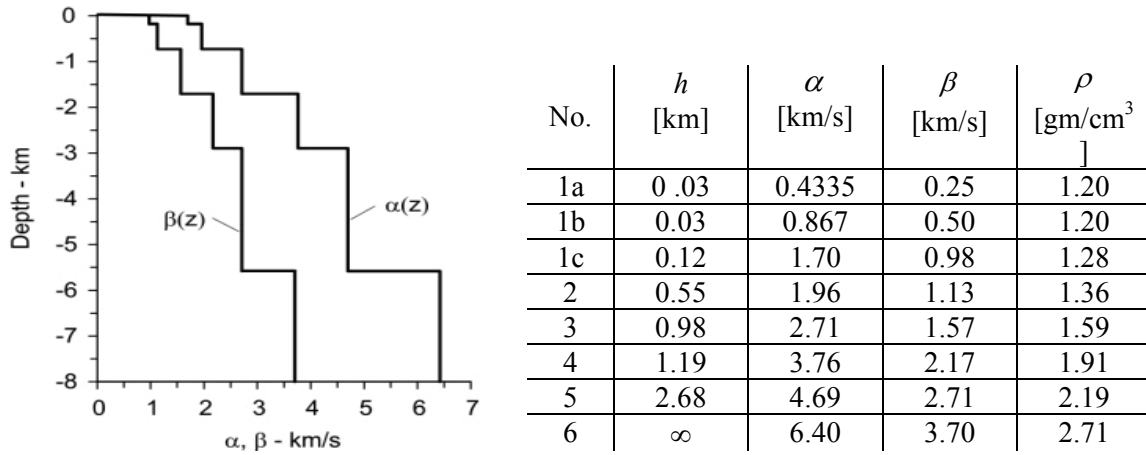


Fig. 3 Site velocity profile for the examples shown in this paper.

Synthetic Motions on an Array of Points

Sites where correlated motions are needed for analysis of extended structures are typically at distances from few tens of meters to few kilometers. It is assumed that the motions at such sites differ only because of deterministic propagation and attenuation due to Q , while the randomness in phase and mode participation factors, included in coefficients A_{nm}^* , are the same. Therefore, the motion at a representative site $x = x_0$ is first synthesized, and the motion at $x = x_0 + \Delta x$ is computed with coefficients $A_{nm}^*(x_0)$ and analytical derivatives of the wavelet. Similarly, representations of the velocities, displacements, strains, rotations and curvatures are obtained analytically in the frequency domain (Todorovska et al., 2013).

$$\hat{u}(x_0 + \Delta x, \omega) = \sum_{n=1}^N \sum_{m=1}^{M_n} A_{nm}^*(x_0) \hat{w}_{nm}(x_0 + \Delta x; \omega) \quad (5)$$

Synthetic Strains and Rotations

The compressional strain is

$$\hat{\varepsilon}_{xx}(x; \omega) = \frac{\partial}{\partial x} \hat{u}_x(x; \omega) \quad (6)$$

and the shear strain is

$$\begin{aligned} \hat{\varepsilon}_{xy}(x; \omega) &= \frac{1}{2} \left[\frac{\partial}{\partial x} \hat{u}_y(x; \omega) + \frac{\partial}{\partial y} \hat{u}_x(x; \omega) \right] \\ &= \frac{1}{2} \frac{\partial}{\partial x} \hat{u}_y(x; \omega) \end{aligned} \quad (7)$$

The point rotations (those of an infinitesimal volume at the point on the ground surface), can be obtained by applying the curl operator on the displacement vector

$$\begin{aligned} \vec{\psi}(x; \omega) &= \nabla \times \vec{u}(x; \omega) \\ &= \begin{vmatrix} \vec{i} & \vec{j} & \vec{k} \\ \frac{\partial}{\partial x} & \frac{\partial}{\partial y} & \frac{\partial}{\partial z} \\ u_x & u_y & u_z \end{vmatrix} \end{aligned} \quad (8)$$

where \vec{i} , \vec{j} and \vec{k} are unit vectors in the x , y and z directions. The nonzero rotations are the torsion

$$\psi_z(x; \omega) \vec{k} = \frac{\partial u_y(x; \omega)}{\partial x} \vec{k} \quad (9)$$

and rocking $\psi_y(x; \omega) \vec{j}$

$$\psi_y(x; \omega) \vec{j} = -\frac{\partial u_z(x; \omega)}{\partial x} \vec{j} \quad (10)$$

Target Spectrum

The target Fourier spectrum can be that of a *scenario* earthquake, generated by one of the built-in empirical scaling models (Trifunac and Lee, 1985; Trifunac, 1976, 1979, 1989a,b), which makes the amplitudes of the generated motion automatically consistent, in a statistical sense, with observation. The target spectrum can also be a *uniform hazard Fourier spectrum*, or any given Fourier spectrum. The built-in scaling models all generate site-specific spectra, and differ in the input parameters. A particular model can be chosen depending on how detailed information is available for the site. For example, earthquake magnitude or Modified Mercalli site intensity can be specified. The local site conditions are described on two scales – geologic and local soil, which sample respectively the geology up to depths of the order of kilometers and hundreds of meters. Fig. 4 illustrates uniform hazard Fourier spectra for a site in Alaska (computed by program NEQRISK, Lee and Trifunac 1985b) for different site conditions. The solid lines show spectra for “soft” condition (deep soil over sediments), and the dashed lines show spectra for “hard” site conditions (rock soil over geologic rock), all for different probabilities p of being exceeded. It is seen that the shape of the spectra depends significantly on the site conditions.

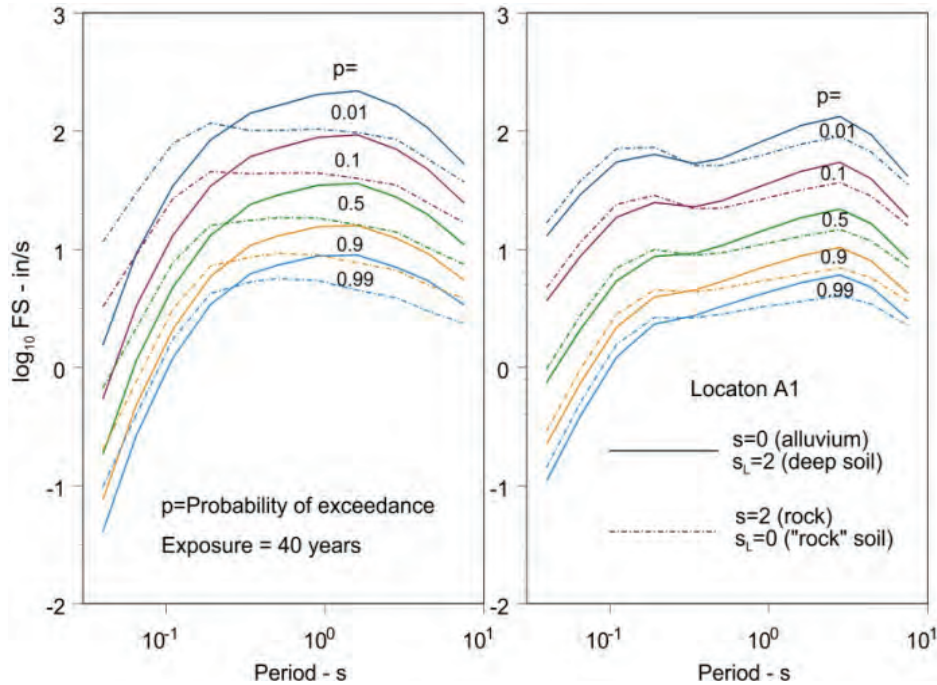


Fig. 4 Example of target Uniform Hazard Fourier spectra for a site near Cook Inlet in Alaska (left: horizontal component; right: vertical component).

RESULTS

The methodology is illustrated for a scenario earthquake. Fig. 5 shows synthetic accelerations, velocities and displacements in the radial, vertical and transverse directions (top) and axial and shear strains (bottom), generated by M6.5 earthquake, at R=10 km hypocentral distance, at a site on soft soil over sediments (corresponding to parameters $s=0$ and $s_L=2$ as defined in Trifunac, 1989b), unfolded with dispersion for the geology profile in Fig. 3. The agreement between the Fourier spectra of the synthetic motion and the target empirical spectra is shown in Fig. 6. Fig. 7 shows an extension of the accelerations (left) and displacements (right) in Fig. 5 to an array of sites 100 m apart in the radial direction for the acceleration and 1 km apart for the displacements. Noticeable differences in the acceleration time histories can be seen even though the sites are very close to each other. The differences, created by a purely deterministic physical model of wave propagation, are more complex than single phase shift and some small amplitude decay, as assumed in the engineering stochastic methods. The displacements exhibit higher degree of similarity in waveforms even at distances several kilometers away, but their difference is not a simple shift in time. Finally, Fig. 8 shows the same quantities as Fig. 5 but for a larger and more distant earthquake (M7.5 and R=100 km).

CONCLUSIONS

The SYNACC method for generation of multi-component synthetic time histories of earthquake ground motion at an array of points on the ground surface was reviewed. Such motions are needed for design of long structures, such as pipelines, tunnels and bridges, and in particular for nonlinear analyses in the time domain. The method produces site specific and realistic time histories with amplitudes and spectral content that are consistent, in a statistical sense, with observations over the frequency band of interest for engineering applications (0-25 Hz), when the target spectrum is generated by empirical scaling equations.

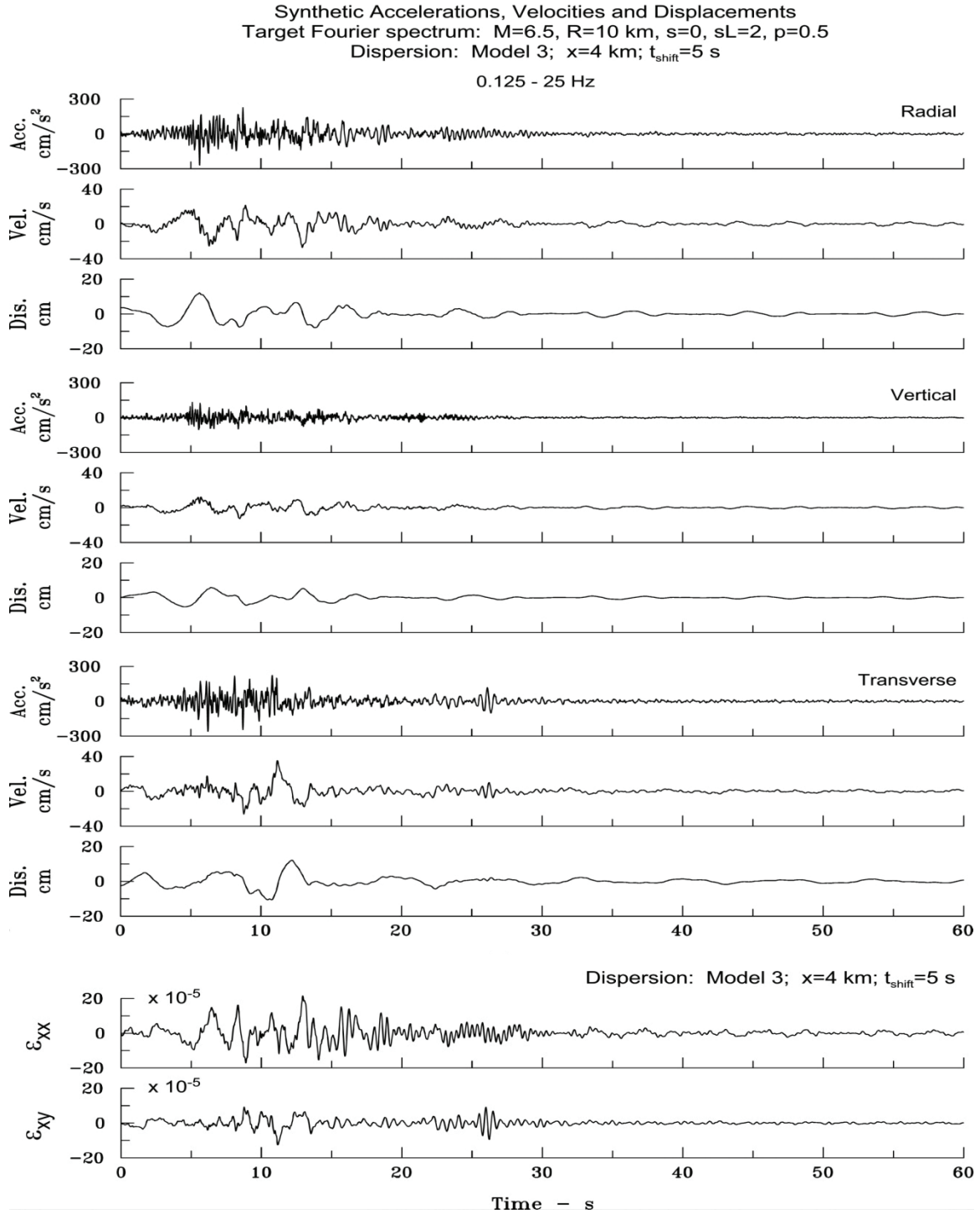


Fig. 5 Top: Synthetic acceleration, velocity and displacement for the radial, vertical and transverse component of motion, computed for target Fourier spectrum that corresponds to M6.5 earthquake, at hypocentral distance $R=10$ km, and for a site on sediments ($s=2$) and deep soil ($s_L=2$), unfolded with dispersion model 3 (see Fig. 3). Bottom: The corresponding axial and shear strains, ϵ_{xx} and ϵ_{xy} . (Redrawn from Todorovska et al., 2013).

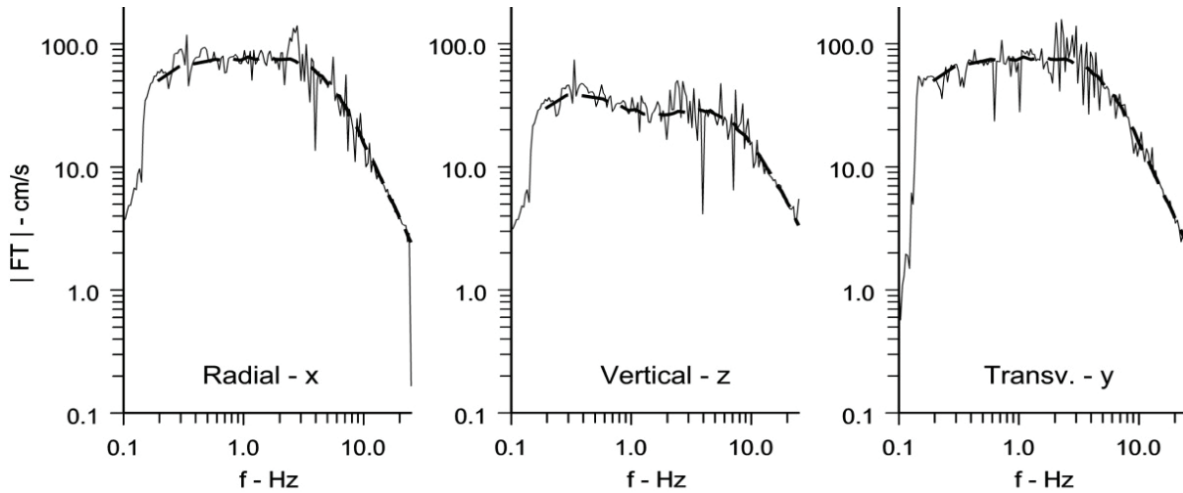


Fig. 6 Agreement of the Fourier spectra of acceleration of the synthetic motions in Fig. 5 (solid line) with the corresponding empirical target spectra used to generate the synthetic motions (dashed line). (Redrawn from Todorovska et al., 2013).

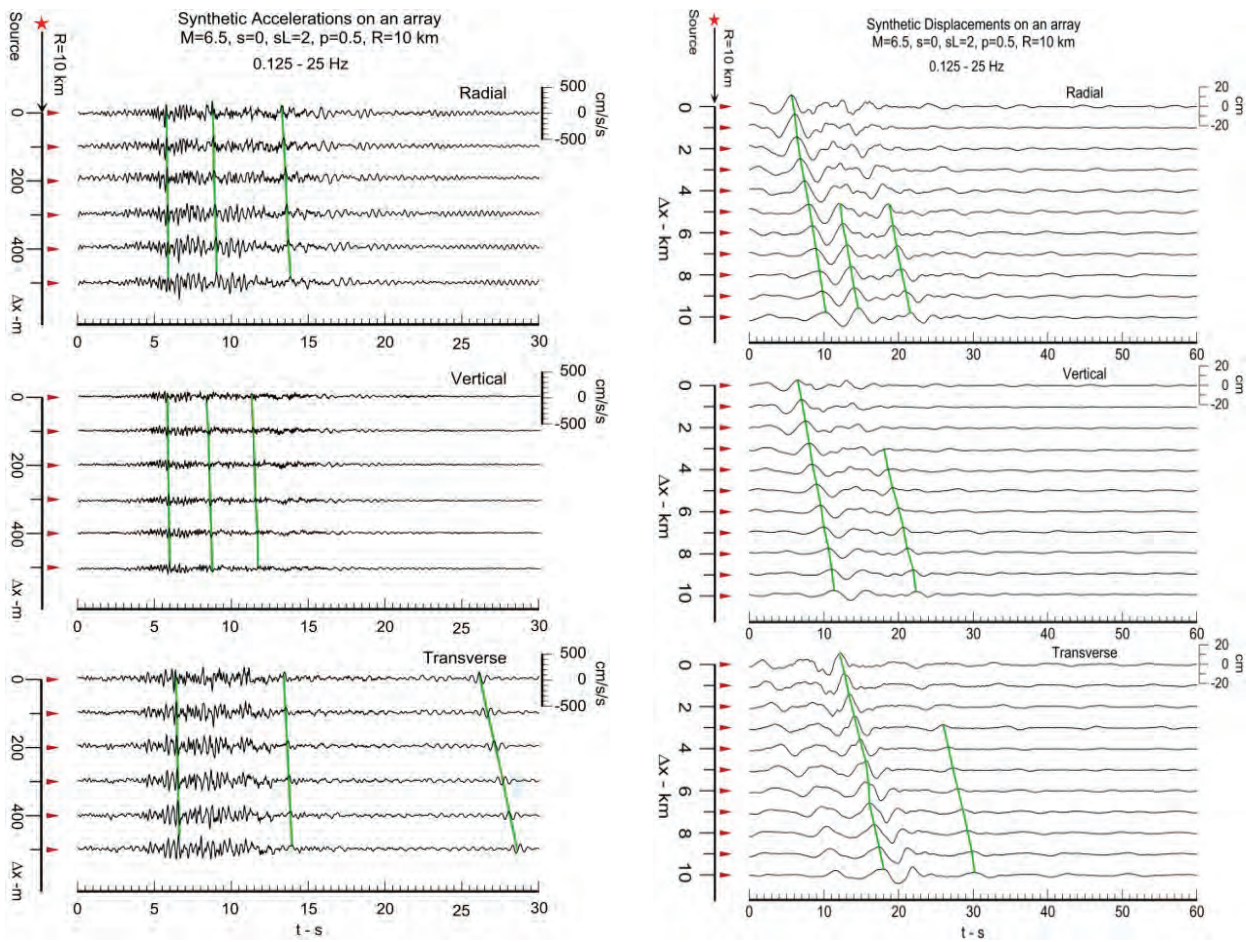


Fig. 7 Synthetic radial, vertical and transverse accelerations (left) at 6 sites 100 m apart, and displacements (right) at 11 sites, 1 km apart, for M6.5 earthquake, at distance 10 km from the closest site. (Redrawn from Todorovska et al., 2013).

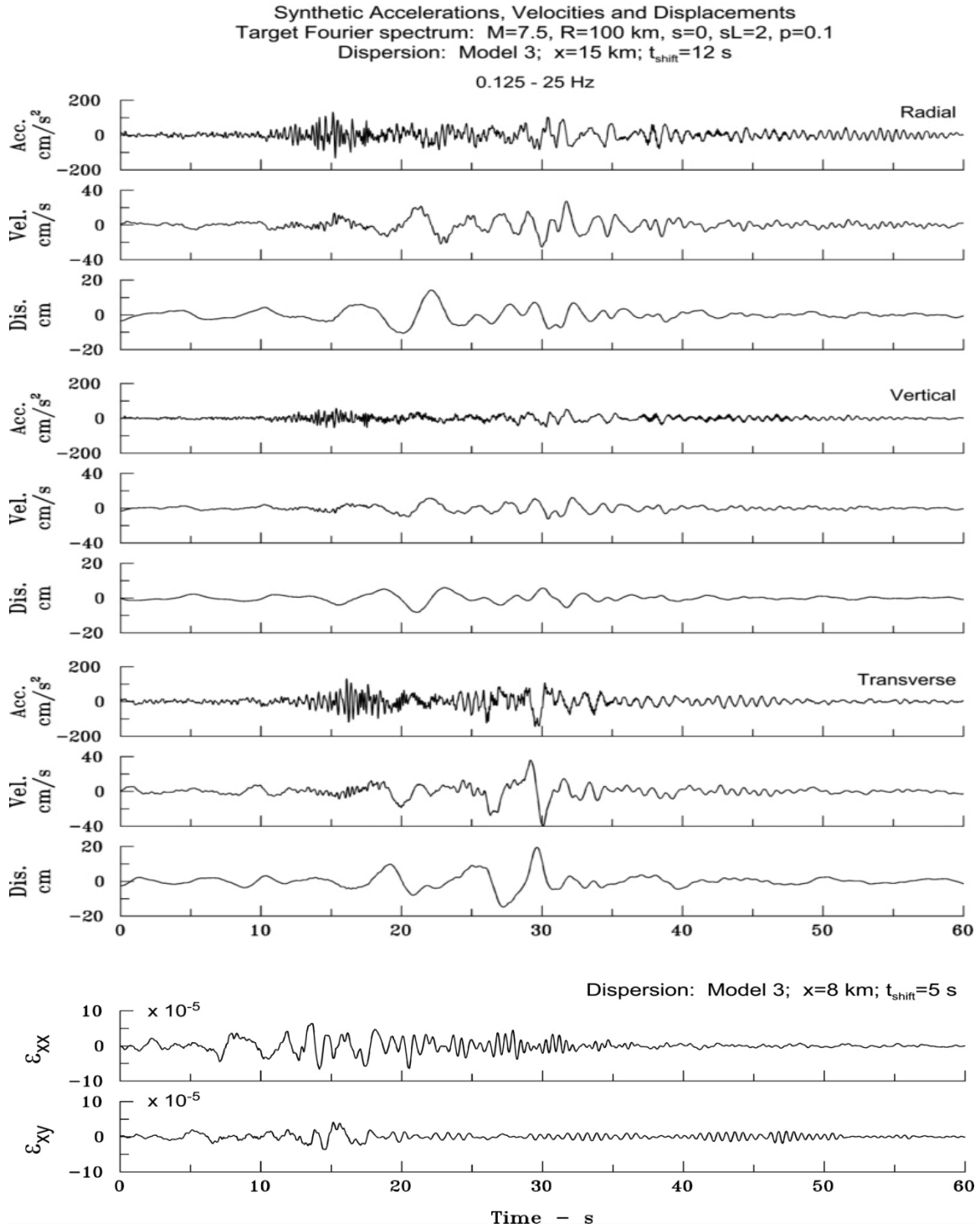


Fig. 8 Top: Synthetic acceleration, velocity and displacement for the radial, vertical and transverse component of motion, computed for target Fourier spectrum that corresponds to M7.5 earthquake, at hypocentral distance $R=100$ km, and for a site on sediments ($s=2$) and deep soil ($s_L=2$), unfolded with dispersion model 3 (see Fig. 3). Bottom: The corresponding axial and shear strains, ϵ_{xx} and ϵ_{xy} . (Redrawn from Todorovska et al., 2013).

ACKNOWLEDGEMENTS

The work presented in this paper was supported in part by the Canadian Nuclear Safety Commission (CNSC). This support is gratefully acknowledged.

REFERENCES

- Haskell NA (1953). The dispersion of surface waves in multilayered media, *Bull. Seism. Soc. Am.*, **43**, 17-34.
- Lee VW (1990). Surface strains associated with strong earthquake shaking, *Proc. J.S.C.E.*, 422(n I-14), 187-194.
- Lee VW (2002). Empirical scaling of strong earthquake ground motion - Part III: Synthetic Strong Motion, *ISET J. of Earthquake Technology*, Paper No. 427, **39**(4), 273-310.
- Lee VW, Trifunac MD (1985a). Torsional accelerograms, *Int. J. Soil Dyn. Earthq. Eng.*, **4**(3), 132-139.
- Lee VW, Trifunac MD (1985b). Uniform risk spectra of strong earthquake ground motion. Report No. 85-05, Dept. of Civil Engrg., U. So. California, Los Angeles, California.
- Lee VW, Trifunac MD (1987). Rocking strong earthquake accelerations, *Int. J. Soil Dyn. Earthq. Eng.*, **6**(2), 75-89.
- Todorovska MI, Trifunac MD, Lee VW, Orbović N (2013). Synthetic earthquake ground motions on an array, *Soil Dyn. Earthq. Eng.*, **48**, 234-251.
- Trifunac MD (1971). A method for synthesizing realistic strong ground motion, *Bull. Seism. Soc. Amer.*, **61**, 1739-1753.
- Trifunac, MD. (1976). Preliminary empirical model for scaling Fourier amplitude spectra of strong ground acceleration in terms of earthquake magnitude, source to station distance and recording site conditions, *Bull. Seism. Soc. Amer.*, **66**, 1343-1373.
- Trifunac, MD. (1979). Preliminary empirical model for scaling Fourier amplitude spectra of strong motion acceleration in terms of Modified Mercalli Intensity and geologic site conditions, *Earthq. Engng Struct. Dynam.*, **7**, 63-74.
- Trifunac MD. (1989a). Dependence of Fourier spectrum amplitudes of recorded strong earthquake accelerations on magnitude, local soil conditions and on depth of sediments, *Earthq. Eng Struct. Dyn.*, **18**(7), 999-1016.
- Trifunac MD (1989b). Scaling of Fourier spectrum amplitudes of recorded strong earthquake accelerations in terms of magnitude and local soil and geologic conditions, *Earthq. Eng Vib.*, **9**(2), 23-44.
- Trifunac MD (1990). Curvograms of strong ground motion, *ASCE, EMD*, **116**(6), 1426-1432.
- Trifunac MD (1994). Q and high frequency strong motion spectra, *Soil Dyn. Earthq. Eng.*, **13**(3), 149-161.
- Trifunac MD, Lee VW (1985). Preliminary empirical model for scaling Fourier amplitude spectra of strong ground acceleration in terms of earthquake magnitude, source to station distance, site intensity and recording site conditions, Report CE 85-03, Dept. of Civil Eng., U. So. California, Los Angeles, California.
- Wong HL, Trifunac MD (1978). Synthesizing realistic strong motion accelerograms, Report No. 78-07, Dept. of Civil Engrg., U. of So. California, Los Angeles, California.
- Wong HL, Trifunac MD (1979). Generation of artificial strong motion accelerograms, *Int. J. Earthquake Eng. Struct. Dynamics*, **7**, 509-527.
- Zerva A. (2009). Spatial variation of seismic ground motions: modeling and engineering applications. CRC Press, Taylor and Francis Group, Boca Raton, Florida.